Building Material Recognition and Feature Extraction Using Small CCD Sensor and Image Analysis and Clustering Techniques

Stefano Pagnotta [1*], Danis Ionut Filimon [2], Gianni Gallello [3], Marco Lezzerini [4]

[1*] Department of Earth Sciences, University of Pisa, Via S. Maria 53 - 56126, Pisa, Italy; email: stefano.pagnotta@unipi.it, https://orcid.org/0000-0002-6645-4924

[2] Department of Earth Sciences, University of Pisa, Via S. Maria 53 - 56126, Pisa, Italy

[3] Department of Prehistory, Archeology and Ancient History University of Valencia Av. Blasco Ibáñez 28 - 46010, Valencia, Spain; email: gianni.gallello@uv.es; https://orcid.org/0000-0003-3641-8815

[4] Department of Earth Sciences, University of Pisa, Via S. Maria 53 - 56126, Pisa, Italy; email: marco.lezzerini@unipi.it; https://orcid.org/0000-0001-9204-4462

http://doi.org/10.29227/IM-2024-01-25

Submission date: *27.4.2023* | Review date: *19.5.2023*

Abstract

Heritage Building material recognition is the process of classifying building materials based on their visual appearance. It is important in construction, urban planning, and archaeology. Image analysis is a common approach, starting with acquiring RGB images, then extracting features using techniques such as colour histograms and texture analysis, and clustering the materials into groups using algorithms like k-means. Finally, the materials are classified into categories using classifiers like decision trees, SVM, or neural networks. Image analysis is a useful tool for building material recognition, as it allows for accurate classification of building materials based on their visual characteristics.

Keywords: material recognition, building material, feature extraction, ccd sensor, image analysis, clustering techniques

Introduction

Building material recognition is the process of identifying and classifying different materials used in construction based on their visual appearance [1]. This task is critical in various fields such as construction, urban planning, and archaeology, as it provides important information about the composition of buildings and structures. With the development of artificial intelligence and the increasingly urgent need to allow these entities to autonomously recognize not only forms but also materials, research dedicated to implementing these methods is making giant steps [2].

The common approach to building material recognition is through Image Analysis, where an image of a building or a portion of it, named Region of Interest (ROI), is captured, and processed to extract features that can be used to classify all the building materials present in it. The process starts with acquiring RGB (Red, Green, and Blue channels) images, which provide a rich representation of the visual characteristics of each building material [3]. Next, various image pre-processing and processing techniques such as colour histograms, texture analysis, or edge detection are applied to extract features that can distinguish among different building materials. These techniques help to identify the unique characteristics of each material, such as its colour, texture, and shape. The extracted features are then used to cluster the building materials into different groups using algorithms such as k-means, hierarchical clustering, density-based clustering, and artificial intelligence clustering. The choice of algorithm depends on the nature of the data and the specific requirements of the application [3–5].

Finally, the building materials are classified into different categories based on their features, a process known as material classification. Various classifiers can be used, including decision trees, support vector machines (SVM), and neural networks. The choice of classifier depends on the nature of the data and the specific requirements of the application [4–6]. Pagnotta et al. [7–11] have experimented in various application fields the potentialities of using image analysis in the field of cultural heritage and geological material analysis, both at the macro and micro scale, using different image data acquisition sources. Lee et al. [12] report a critical review on the use of smartphones in the field of geosciences, analyzing their future perspectives, while Daffara et al. [13] show some specific applications of these devices in the field of cultural heritage. Ramacciotti et al. [14] used smartphone imaging combined with other analytical techniques to allow the classification of different types of building mortars present in the Torre de Silla (Spain) and in the Fuengirola's castle (Spain). This work represents a very specific application of using only a small CCD sensor, equipped on a commercial smartphone, for scientific and analytical purposes. In this work, we want to explore the possibility of using such kind of device sensors, such as those mounted on smartphones, gimbal camera and small drones, which are increasingly widespread in the field of documentation for cultural heritage, to distinguish between different types of geomaterials due to their colour features and textures. Furthermore, we want to test the ability to distinguish colour alterations that are due to natural and environmental degradation of the rock. In this work, we tested the effectiveness of a small-scale CCD sensor mounted on a mid-range commercial smartphone, for the segmentation of different materials present in a portion of the masonry of the church of S. Paolo in Ripa d'Arno. The ROI image was processed using the Otsu grayscale tresholding algorithm [15], the triangle method [16] and k-means [17] clustering on the pre-processed RGB image only. For the implementation of the artificial intelligence, a self-organized Kohonen network (SOM) was used, carrying out a further processing of the primary image [18], performing colour space transformations and extracting other information such as entropy [19], standard deviation [20] and pixel

range [21], useful for reinforcing the input data to the neural network. The first results show how these small sensors can be efficient in recognizing different materials, with very large chromatic variations, and some forms of their degradation due to the nature of the rock and their interaction with the surrounding environment.

Material and Methods

For the purposes of this work, we selected the façade of S. Paolo in Ripa d'Arno Church, a historical and cultural interest building located in the urban circuit of Pisa. Given the nature of this work as a first approach, once the building was selected, we proceeded with the selection of a ROI on which to conduct our experiment (Fig. 1). All procedures were carried out using a script created in the MATLAB environment. The photos of the case study were taken using a smartphone, equipped with a multi-sensor camera (108MP + 8MP + 2MP), REDMI Note 11 pro 5g. It uses a 108MP Samsung ISOCELL HM2 1/1.52" sensor with 0.7µm pixels and 24mm f/1.9 lens. Small-sized CCD sensors like this are now equipped on many devices, from smartphones to gimbal cameras to low-weight drones (<250 g). The images were captured in a single shot using the settings chosen by the onboard AI. The images have not undergone any type of processing to balance the white and the electronic noise of the sensor. We have chosen to simulate the normal use of a camera of this type (point and click) operated by a non-expert user. Subsequently, the images were subjected to a preliminary correction of the perspective and to a cropping. The preprocessed images were visualized, and a single image was chosen to be processed through the MATLAB script. We chose to work on a ROI chosen for the presence of two main types of geomaterials which also had forms of color alteration due to the nature of the rock and the interaction with the environment. The PC used for image processing is an Asus ROG Zephyrus G14 equipped with an AMD Ryzen 7 4000 series processor, with 32 GB RAM and a Nvidia Geforce RTX video card with 6 GB dedicated RAM. The entire processing of the images took 15 minutes and fifty-five seconds (15':55") with five hundred repetitions of the algorithm (epoch).

The pre-processed image is loaded into a MATLAB script, where it is converted into the HUE and CIE Lab* color spaces. After this step, the three resulting images are decomposed into individual constituent channels, resulting in a dataset of 12 images. To further increase the input space for subsequent artificial intelligence (AI) processing, we calculated the images for entropy (E), standard deviation (S), and pixel range (R). The primary RGB image is segmented using the Otsu algorithm [22] and the triangle method [15]. Subsequently, a peak finding algorithm is used on the grayscale image histogram, which will determine the number of clusters to be used for the K-Means segmentation [17]. The twelve images, which represent an expansion of the original R^3 space into R^{12}, are used as reinforced input for a SOM neural network that will further reduce the space to R^4, this is because the histogram analysis performed for the SOM has identified the existence of four main clusters of features (Fig. 2). The results obtained are analyzed and compared.

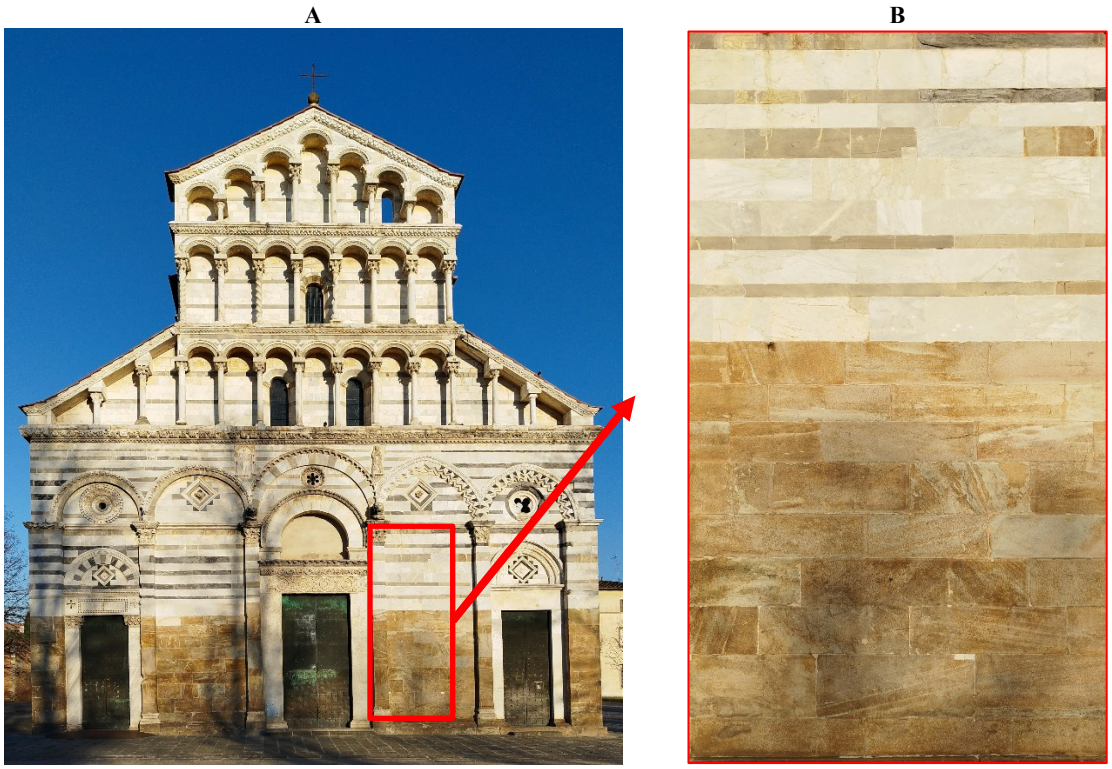

Fig. 1. Image of the façade of S. Paolo in Ripa d'Arno with selected ROI (A) and selected ROI (B).

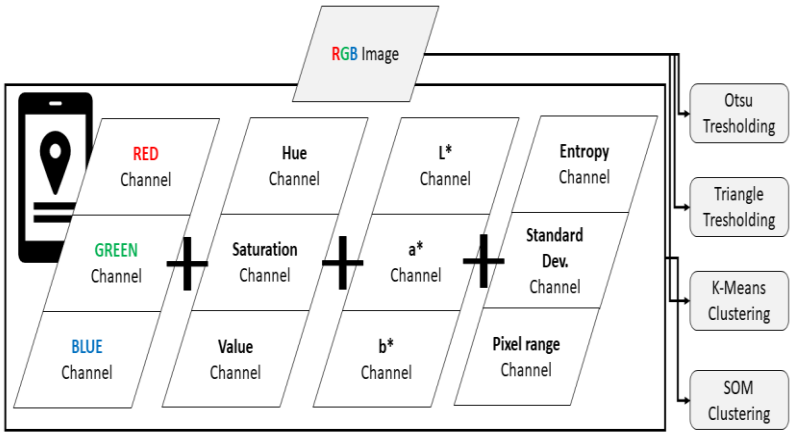

Fig. 2. Conceptual scheme of the MATLAB script elaboration.

The SOM network was implemented using twelve images as input. The dataset consists of nine images obtained from RGB, the HUE, CIE L*a*b* color space, entropy, local standard deviation and pixel range (Fig. 3).

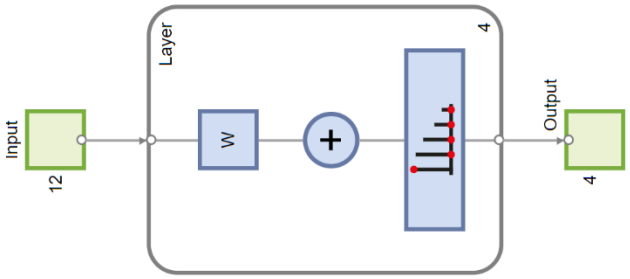

Fig. 3. Structure of the SOM neural network with 12 input images and 4 output segments ($R^{12} \rightarrow R^4$).

As a result of using the SOM type neural network, we obtained 4 segments consisting of logical values (0 and 1, where 0 indicates the absence of pixels and 1 their presence). These segments topologically represent the areas where a given feature is present.

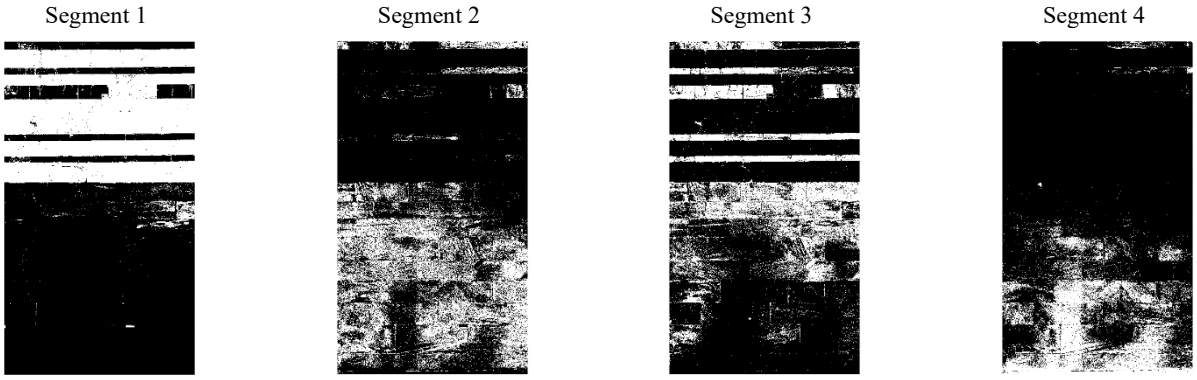

Fig. 4. Segments produced from SOM clustering.

We know from the De Bodt et alii [23] that the random assignment of the initial weights and centroids has no influence on the reproducibility of the SOM networks. However, we have devised an empirical method to summarily estimate the reproducibility of the network: we repeated the SOM segmentation ten times in a row on the same dataset, choosing a fixed set of ten control pixels that fell within the clusters (4) and at the edge of the clusters (6): for the pixels inside the cluster areas there were no assignment errors (cluster assignment variation), while for those at the edges of the cluster there was one assignment error out of ten trials carried out.

Results and Discussions

The result obtained by imposing a threshold value in the grey scale, both with the Otsu method and with the triangle method, was not satisfactory in our case. The chromatic variation was not clear enough to allow a threshold that would allow to distinguish between the two geomaterials present. (Fig. 5)

Fig. 5. Results of the tresholding methods: original image (left); triangle method tresholding (center); Otsu Tresholding method (right).

Using the histogram of the grayscale image to implement an automatic selection of the number of k to be used for the k-means algorithm produced a better result in terms of the number of features identified within the ROI. This made it possible to automatically identify two main geomaterials and a colour alteration for one of them, for a total of three identified features. (Fig. 6)

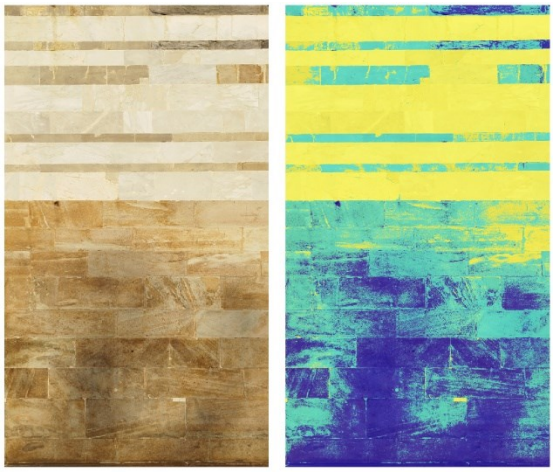

Fig. 6. Results of the K-Means clustering. The original image (Left). The K-Means clustering (Right): limestones (yellow); sandstones (cyan); colour alteration of the sandstones (blue).

Clustering using the k-mean method combined with an algorithm for automatic identification of the number of clusters to assign, allowed the two materials to be well separated. There are some inaccuracies probably due to colour variations caused by problems of over/under exposure of the image and/or light reflections. In the portion belonging to the sandstones, there are portions (in yellow) identified as belonging to the limestones, but which are, in reality, points in which the material has lighter tones and close to those typical of limestones.

The use of the SOM-type artificial neural network has allowed to increase the detail of the clustering, while still maintaining a certain level of imprecision (Fig. 7). In the sandstones, there is still a small area classified as limestone, which is a sandstone that has a very light colour.

Fig. 7. The SOM clustering results (on the right) compared to the original ROI (on the left). Green = Segment 1; brown = Segment 2; blue = Segment 3; cyan = Segment 4.

The advantage of this type of system lies in the fact that it automatically produces separate images of the areas as seen in the Fig. 4, which have logical values and can be automatically translated into vectorial data useful to produce documentation for

restoration [24]. Even if not very precise, the method can produce in a short time and in an automated/semi-automated way useful information for professionals to verify, for example, the homogeneity of the chromatic rendering of a restoration intervention or even the degree of compatibility between the colours of original and restoration materials. At the same time identifying the relative percentage of portions of the masonry in which the chromatic difference is very high (Tab. *1*), even within the same material, which can compromise the correct reading of the monument from the point of view of the materials, when not observed closely. On the scale of images taken with the smartphone camera, it is possible to automatically recognize the presence of two geologic materials: limestone falls within segment 1, while sandstones and their surface alterations fall within segments 2, 3, and 4. However, it should be noted that surface alterations of sandstones, which appear very light, are assigned by artificial intelligence to segment 1. By performing a manual validation check of the results, we estimated that the error rate of automatic material recognition is approximately 1%.

Tab. 1. Relative percentage of pixel area occupied by single segments.

Segments	Area in pixel (%)
Seg1	33
Seg2	26
Seg3	24
Seg4	17

If we consider Tab. *1* and Fig. 7, we can observe that segment 1 covers 33% (±1) of the ROI area, while the area occupied by the second geologic material is given by the sum of segments two to four (67%±1) of this area. Of this, 38.81% (±1) exhibits a greyish-brown alteration colour, 35.82% (±1) represents an unaltered surface, likely restored, and 25.37% (±1) exhibits a strong darkening.

Conclusions

In the era of miniaturization and portable devices with large computing capacity and that are increasingly equipped with artificial intelligence systems to perform various functions, think about the possibility of implementing algorithms and AI dedicated to scientific analysis on some of these devices, might not be so wrong. Several researchers are already working on the possibilities offered by small format CCD sensors in image analysis in various fields of application. Our experiment demonstrates in a simple way that these devices have enormous potential both when coupled with classical methods of image analysis and when coupled with innovative algorithms such as those of artificial intelligence. In our case, we were able to distinguish and map the presence of two different materials, which also present chromatic alterations due to the natural degradation of the rock and/or to the degradation produced by the interaction between the rock and the surrounding environment. Furthermore, it was possible to quantify the relative areas occupied by each geomaterial in the ROI and make some qualitative considerations on the state of degradation and conservation of the exposed surfaces.

References

1. X.-W. Ye, C.-Z. Dong, T. Liu, A review of machine vision-based structural health monitoring: methodologies and applications, J. Sensors. 2016 (2016).
2. M. Egmont-Petersen, D. de Ridder, H. Handels, Image processing with neural networks—a review, Pattern Recognit. 35 (2002) 2279–2301.
3. R.M. Haralick, L.G. Shapiro, Image segmentation techniques, Comput. Vision, Graph. Image Process. 29 (1985) 100–132.
4. H. Zhang, J.E. Fritts, S.A. Goldman, Image segmentation evaluation: A survey of unsupervised methods, Comput. Vis. Image Underst. 110 (2008) 260–280.
5. N. Senthilkumaran, R. Rajesh, Image segmentation-a survey of soft computing approaches, in: 2009 Int. Conf. Adv. Recent Technol. Commun. Comput., IEEE, 2009: pp. 844–846.
6. P. Geladi, H.F. Grahn, Multivariate image analysis, Encycl. Anal. Chem. Appl. Theory Instrum. (2006).
7. L. Santoro, M. Lezzerini, A. Aquino, G. Domenighini, S. Pagnotta, A Novel Method for Evaluation of Ore Minerals Based on Optical Microscopy and Image Analysis: Preliminary Results, Minerals. 12 (2022) 1348. https://doi.org/10.3390/min12111348.
8. S. Pagnotta, A. Aquino, M. Lezzerini, Image Segmentation for Reflected-Light Microscopy: Some Theoretical Approaches, in: IOP Conf. Ser. Earth Environ. Sci., IOP Publishing, 2021: p. 12121.
9. G.S. Senesi, B. Campanella, E. Grifoni, S. Legnaioli, G. Lorenzetti, S. Pagnotta, F. Poggialini, V. Palleschi, O. De Pascale, Double-pulse micro-laser-induced breakdown spectroscopy applied tothree dimensional mapping of stonemonumentsamples, in: IMEKO Int. Conf. Metrol. Archaeol. Cult. Heritage, MetroArchaeo 2017, 2019.
10. S. Pagnotta, S. Legnaioli, B. Campanella, E. Grifoni, M. Lezzerini, G. Lorenzetti, V. Palleschi, F. Poggialini, S. Raneri, Micro-chemical evaluation of ancient potsherds by μ-LIBS scanning on thin section negatives, Mediterr. Archaeol. Archaeom. 18 (2018) 171–178. https://doi.org/10.5281/zenodo.1285906.
11. S. Pagnotta, M. Lezzerini, B. Campanella, G. Gallello, E. Grifoni, S. Legnaioli, G. Lorenzetti, F. Poggialini, S. Raneri, A. Safi, V. Palleschi, Fast quantitative elemental mapping of highly inhomogeneous materials by micro-Laser-Induced Breakdown Spectroscopy, Spectrochim. Acta - Part B At. Spectrosc. 146 (2018). https://doi.org/10.1016/j.sab.2018.04.018.
12. S. Lee, J. Suh, Y. Choi, Review of smartphone applications for geoscience: current status, limitations, and future perspectives, Earth Sci. Informatics. 11 (2018) 463–486.
13. C. Daffara, G. Marchioro, D. Ambrosini, Smartphone diagnostics for cultural heritage, in: Opt. Arts, Archit. Archaeol. VII, SPIE, 2019: pp. 260–270.
14. M. Ramacciotti, G. Gallello, M. Lezzerini, S. Pagnotta, A. Aquino, L. Alapont, J. Antonio Martín Ruiz, A. Pérez-Malumbres Landa, R. Hiraldo Aguilera, D. Godoy Ruiz, A. Morales-Rubio, M. Luisa Cervera, A. Pastor, Smartphone application for ancient mortars identification developed by a multi-analytical approach, J. Archaeol. Sci. Reports. 43 (2022). https://doi.org/10.1016/j.jasrep.2022.103433.
15. P.D.R. Raju, G. Neelima, Image segmentation by using histogram thresholding, Int. J. Comput. Sci. Eng. Technol. 2 (2012) 776–779.
16. G.W. Zack, W.E. Rogers, S.A. Latt, Automatic measurement of sister chromatid exchange frequency., J. Histochem. Cytochem. 25 (1977) 741–753.
17. N. Dhanachandra, K. Manglem, Y.J. Chanu, Image segmentation using K-means clustering algorithm and subtractive clustering algorithm, Procedia Comput. Sci. 54 (2015) 764–771.
18. T. Kohonen, The self-organizing map, Neurocomputing. 21 (1998) 1–6.
19. C. Thum, Measurement of the entropy of an image with application to image focusing, Opt. Acta Int. J. Opt. 31 (1984) 203–211.
20. D.-C. Chang, W.-R. Wu, Image contrast enhancement based on a histogram transformation of local standard deviation, IEEE Trans. Med. Imaging. 17 (1998) 518–531.
21. A. Ranganath, M.R. Senapati, P.K. Sahu, Estimating the fractal dimension of images using pixel range calculation technique, Vis. Comput. 37 (2021) 635–650.
22. N. Otsu, A threshold selection method from gray-level histograms, IEEE Trans. Syst. Man. Cybern. 9 (1979) 62–66.

23. E. De Bodt, M. Cottrell, M. Verleysen, Statistical tools to assess the reliability of self-organizing maps, Neural Networks. 15 (2002) 967–978.

24. A. Amura, A. Aldini, S. Pagnotta, E. Salerno, A. Tonazzini, P. Triolo, Analysis of Diagnostic Images of Artworks and Feature Extraction: Design of a Methodology, J. Imaging. 7 (2021) 53.